**Professor Ray Clough coined the finite element terminology** in the publication "The Finite Element Method in Plane Stress Analysis", Proceedings, Second Conference on Electronic Computation, ASCE, in Pittsburgh, PA, Sept. 1960. At that time, the vacuum-tube IBM 701 could only solve 40 equations; therefore, the examples presented were small and the engineer had to develop the stiffness matrix by hand calculations. During the next year, graduate student Ed Wilson, working under the direction of Ray Clough, developed (on the IBM 704) the first completely automated finite element program that could analyze any plane stress structure without program modification or the requirement to perform additional hand calculations.

The first application of the program clearly demonstrated the significant power of the Finite Element Method, FEM, in solving a very complex real problem in the repair of Norfork Dam. The resulting publication in the Bulletin RILEM[3], a group of international laboratories and experts in materials and analysis of structures. The recognition by this large and respected international group of structural engineers was one of the major reasons the FEM was accepted within a few years. Prior to 1963, experimental physical models, photo-elasticity and finite differences analyses methods were used to solve problems of this type. Within the next several years, most of these methods were replaced by the FEM. *(continued on last page)*

---

# Stress analysis of a gravity dam by the finite element method

R. W. CLOUGH (1) AND E. L. WILSON (2)

RÉSUMÉ

Des études préalables ont montré que la méthode de l'élément fini est un instrument très adapté à l'analyse des états plans de contrainte. Dans la présente communication on décrit l'application de cette méthode à l'analyse de contraintes dans un barrage poids. On a généralisé le programme de la calculatrice digitale de façon à pouvoir tenir compte automatiquement des contraintes thermiques, de celles dues aux poids propre ainsi que des surcharges arbitraires et aussi de façon à pouvoir faire l'analyse par un procédé d'itération. On présente les résultats obtenus pour différentes hypothèses de chargement afin de montrer l'efficacité de la méthode.

SUMMARY

*In previous studies, the finite element method has been shown to provide a convenient tool for the analysis of plane stress systems. The present paper is concerned with the application of this method to stress analysis of a gravity dam. The digital computer program has been extended to account automatically for thermal and dead weight stresses as well as arbitrary live loads, and makes use of an iteration procedure in performing the analysis. Results are described for a number of different loading conditions to demonstrate the effectiveness of the procedure.*

## INTRODUCTION

The matrix algebra formulation of the equations of structural analysis completely generalizes the analytical procedures, and greatly broadens the scope of their applicability. Traditionally, use of the standard methods of structural analysis has been restricted to the treatment of structures built up from one-dimensional members, i.e. members whose elastic and geometric properties can be expressed as functions of position along the elastic axis. Through the use of matrix procedures, however, the same basic principles can be applied in the analysis of entirely different types of structures-comprising assemblages of two-dimensional elements. Included among such structures might be plates, shells, and systems subjected to plane stress or plane strain.

The purpose of this paper is to describe the application of matrix structural analysis methods to the solution of a plane stress elasticity problem. The

(1) Professor of Civil Engineering, University of California, Berkeley, California, U.S.A.

(2) Graduate student, University of California, Berkeley, California, U.S.A.

(3) RILEM - **R**eunion **I**nternationale des **L**aboratoires et **E**xperts des **M**ateriaux was formed in 1948.

general procedure, which is known as the finite element method, has been described in a previous publication[1]. However, although the versatility and range of accuracy of the method were indicated in that report, its usefulness in solving large-scale, practical problems had not yet been demonstrated. For this reason, the authors were pleased to be given the opportunity of undertaking the investigation described in this report: the application of the finite element method to the analysis of stresses and displacements in a large concrete gravity dam. The investigation was sponsored by the Little Rock District Office of the U. S. Army Corps of Engineers, and a complete report: on the studies has been submitted to that office[2]. Due to space limitations, only a brief summary of the work and a representative selection from the final results will be presented here.

## STATEMENT OF THE PROBLEM

The system considered in this investigation was a one foot thick slice of a concrete gravity dam, 196 feet high from the base to the spillway crest, with a profile as shown in figure 1. Of particular interest in the study was the effect on the stress distribution of a crack extending from the foundation rock vertically through most of the height of the section, as shown in the sketch. The loadings to which the structure was sujected included the weight of the concrete, the water pressures, and thermal loads caused by temperature changes (Fig. 2).

Properties assumed for the concrete and for the foundation rock in these analyses are shown in Table I. It will be noted that different moduli of elasticity were assumed for the two materials; the relatively low modulus taken for the concrete was

TABLE I. Assumed properties of materials

| | | |
|---|---|---|
| Concrete: | | |
| Modulus of Elasticity | $E_c$ | $= 2.0 \times 10^6$ psi |
| Poisson's Ratio | $\upsilon$ | $= 0.17$ |
| Unit Weight | $\gamma_c$ | $= 150$ pcf |
| Thermal Coefficient | $\alpha$ | $= 7.0 \times 10^{-6}$ per °F |
| Foundation Rock: | | |
| Modulus of Elasticity | $E_f$ | $= 5.0 \times 10^6$ psi |
| Poissons' Ratio | $\upsilon$ | $= 0.17$ |
| Thermal Coefficient | $\alpha$ | $= 7.0 \times 10^{-6}$ per °F |
| Vertical Modulus (Orthotropic cases) | $E_{fy}$ | $= 1.0 \times 10^6$ psi |
| Water: | | |
| Unit Weight | $\gamma_w$ | $= 62.5$ pcf |

Temperature Change:

$\Delta T = -35°$ F in body of dam decreasing to 0° F about 30 feet below the surface of the foundation rock (Fig. 2).

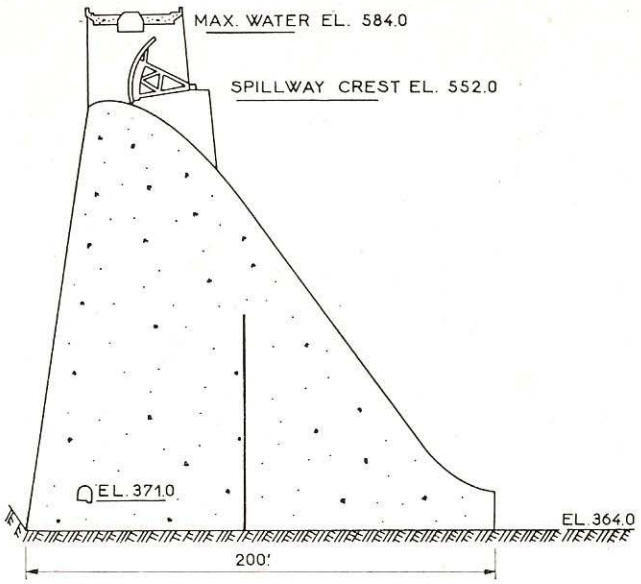


FIG. 1. — **Basic geometry of the dam section.**

intended to account for the effects of creep and plastic flow under sustained load. In one phase of the study, an orthotropic elasticity condition was assumed in the foundation rock (with the vertical modulus only one-fifth of the horizontal) because it is quite possible that horizontal stratification of the foundation might produce such a condition, and it was of interest to determine the resulting effect on the stress distribution in the dam.

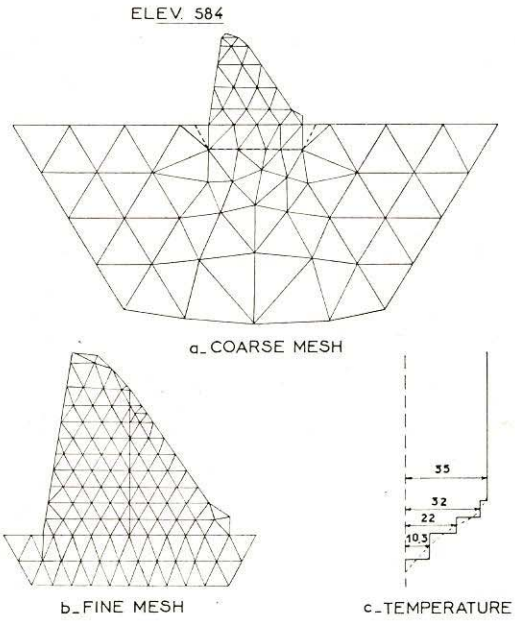


FIG. 2. — **Finite element idealizations of the dam section.**

It was assumed in these studies that the vertical crack resulted from the cooling of the concrete, and the evaluation of the width of the crack opening resulting from each of the various load combinations was one of the principal objects of the studies. In addition, the stress distribution within the section (particularly in the stress concentration zones at the ends of the crack and at the toe and heel of the dam) as well as its overall displacements were of interest. An uncracked section also was studied so that a comparison of the results for the two systems might demonstrate directly the influence of the crack.

## THE FINITE ELEMENT METHOD

Because the finite element method has been described previously, only a brief description of the general features of the method will be given here. In addition, certain features of the present study which have not been presented before will be discussed in greater detail. In general, the method consists of idealizing the actual continuous system as an assemblage of triangular plate elements, interconnected only at the corners, and also loaded only at these points. Within each element, the normal and shear stresses are assumed uniform, thus continuity between the elements is maintained even though they are connected only at the nodal points.

The analysis involves first calculating the stiffnesses of the individual triangular elements; then by adding together the pertinent element stiffnesses, the stiffness of the assembled system is determined. This assembled structure stiffness is represented by the matrix [K] in the equation:

$$\{R\} = [K]\{r\} \tag{1}$$

where also

$\{R\}$ = vector of all nodal point force components
$\{r\}$ = vector of corresponding nodal point displacements.

This equation can be solved formally for the displacements resulting from specified loads by inverting the stiffness matrix. However, in the present study, this matrix was too large to be inverted conveniently, and the displacements were determined from Eq. (1) by an iteration process.

After the nodal point displacements have been obtained, the stress components in each of the triangular elements (which are linearly related to the displacements) can be obtained by the matrix multiplication:

$$\{\sigma\} = [M]\{r\} \tag{2}$$

in which

$\{\sigma\}$ = vector of all element stresses $\sigma_x$, $\sigma_y$, $\tau_{xy}$
$[M]$ = stress transformation matrix.

In this study, the principal stresses in the elements and their directions were also determined, in addition to the $x$, $y$ stresses.

### Element Idealizations

The finite element idealizations used in this study are shown in figure 2. The coarse mesh idealization in figure 2*a* was used in preliminary analyses in order to determine the displacements at the base of the foundation system used in the fine mesh analysis (shown by the dashed line). Thus it was possible to retain the effect of a deep foundation in the fine mesh idealization shown in figure 2*b* without devoting a large number of elements to the foundation zone. It was necessary, of course, to make a separate coarse mesh analysis for each of the loading conditions which were applied to the fine mesh system. In the coarse mesh system, there are a total of 103 elements and 69 nodal points, while in the fine mesh system the numbers are 194 and 130 respectively.

### Element Stiffness

The derivation of the stiffness matrix of an arbitrary isotropic plane stress element is presented in [1], and will not be repeated here. It is of interest to note, however, that this same stiffness matrix can be applied in a plane strain analysis if modified material properties are used, as follows:

$$E^* = \frac{E}{1-\nu^2}$$
$$\nu^* = \frac{\nu}{1-\nu} \tag{3}$$

where $E$ = modulus of elasticity (actual)
$\nu$ = Poissons' ratio (actual)

and the starred values represent the modified properties to be used in a plane strain analysis. The plane stress condition was considered to be more applicable in the present study; but with the assumed value of Poisson's ratio, the difference between the two conditions is negligible: $E^*/E = 1.03$, $\nu^*/\nu = 1.20$.

In order to represent the orthotropic foundation material, it was necessary to develop an orthotropic element stiffness matrix. For this purpose, the stress-strain relationship for an orthotropic material was needed. In this derivation, it was assumed that the orthotropic material actually consisted of a horizontally layered system of alternately hard and soft isotropic materials. Designating the properties of these materials $E_1$, $\nu_1$ and $E_2$, $\nu_2$ respectively, it was further assumed that:

$$\frac{E_1}{\nu_1} = \frac{E_2}{\nu_2} \tag{4}$$

On the basis of these assumptions, the orthotropic stress-strain relationship was found to be

$$\begin{bmatrix} \varepsilon_x \\ \varepsilon_y \\ \gamma_{xy} \end{bmatrix} = \frac{1}{E_x} \begin{bmatrix} 1 & -\nu_x & 0 \\ -\nu_x & \mu & 0 \\ 0 & 0 & 2(\mu + \nu_x) \end{bmatrix} \tag{5}$$

in which

$$E_x = E_1 (1 - r^*); \; r^* = r\left(1 - \frac{E_2}{E_1}\right)$$

$$\nu_x = \nu_1 (1 - r^*)$$

$$\mu = \frac{E_x}{E_y}; \; E_y = \frac{E_2}{r^* + \frac{E_2}{E_1}}$$

and $r$ is the proportion of the total volume occupied by the soft layers. Using this orthotropic stress-strain law, the derivation of the orthotropic element stiffness followed exactly the procedure described in [1] for the isotropic triangular element stiffness.

### Loadings

The load vector $\{R\}$ in Eq. (1) is merely a listing of all the load components applied at the nodal points in any given analysis. For each nodal point, the dead load force was computed by taking one-third of the total weight of all elements attached to the nodal point. Live load (water) forces were applied only at the nodal points in contact with the water, of course, and were taken as the concentrated static equivalent of the distributed water pressures acting on these elements.

The thermal loads were calculated by first determining the stresses which would exist if all strains due to temperature changes were constrained. In a plane stress system, these stresses are given by

$$\sigma = -\frac{E\alpha}{1 - \nu} \Delta T \qquad (6)$$

in which $\alpha$ = thermal coefficient of expansion
$\Delta T$ = change of temperature.

The nodal forces required to maintain these stresses in each element were then found by simple statics. Finally, since these nodal constraints did not really exist, their effect was eliminated by applying equal and opposite nodal forces.

These *reversed* nodal forces are the thermal loads for which the section was analyzed. Displacements resulting from these effective loads are the true thermal displacements in the system. The total thermal stresses were determined by combining the constrained stress of Eq. (6) with the stresses resulting from these thermal loads.

## THE DIGITAL COMPUTER PROGRAM

Practical applications of the finite element method described above require such a tremendous amount of computational effort that they may be performed only by means of automatic digital computers. A special program designed to perform such analyses for arbitrary finite element idealizations has been written for the IBM 704 operated by the University of California Computer Center, and was used in all of the work described in this report.

The computer program performs three major tasks in the complete analysis of a plane stress system. First, the element stiffness and load matrices are formed from a basic numerical description of the structure. Second, Eq. (1) is solved for the displacements of the nodal points by an iteration procedure. Third, the internal element stresses are determined from these displacements. Only the main operations of the computer program will be described here; details of the coding will be omitted. The operation of the program is flexible in that both input and output can be « on-line » or may be effected « off-line » through the use of magnetic tapes and peripheral equipment.

### Numerical Procedure

Before presenting the sequence of operations that is performed by the computer program, it is necessary to discuss in some detail the actual numerical procedure that was employed. This method is a modification of the well-known Gauss-Seidel iteration procedure which, when applied to Eq. (1), involves the repeated calculation of new displacements from the equation

$$r_n^{(s+1)} = (k_{nn})^{-1} \left[R_n - \sum_{i=1, n-1} k_{ni} r_i^{(s+1)} - \sum_{i=n+1, N} k_{ni} r_i^{(s)}\right] \qquad (7)$$

where $n$ = number of the displacement component
$s$ = cycle of iteration

The only modification of the procedure introduced in this analysis is the application of Eq. (7) simultaneously to both components of the displacement at each nodal point. Therefore $r_n$ and $R_n$ become vectors with $x$ and $y$ components, and the stiffness coefficients are in the form

$$k_{lm} = \begin{bmatrix} k_{xx} & k_{xy} \\ k_{yx} & k_{yy} \end{bmatrix}_{lm} \qquad (8)$$

in which $l$ and $m$ are nodal point numbers.

### Over-Relaxation Factor

The rate of convergence of the Gauss-Seidel procedure can be greatly increased by the use of an over-relaxation factor [3]. However, in order to apply this factor it is first necessary to calculate the change in the displacement of nodal point $n$ between cycles of iteration:

$$\Delta r_n^{(s)} = r_n^{(s+1)} - r_n^{(s)}. \qquad (9)$$

The substitution of Eq. (7) into Eq. (9) yields for the change in displacement

$$\Delta r_n^{(s)} = (k_{nn})^{-1} \left[R_n - \sum_{i=1, n-1} k_{ni} r_i^{(s+1)} - \sum_{i=n; N} k_{ni} r_i^{(s)}\right] \qquad (10)$$

The new displacement of nodal point $n$ is then determined from the following equation:

$$r^{(s+1)} = r_{nn}^{(s)} + \beta \Delta r_n^{(s)} \qquad (11)$$

It was assumed in these studies that the vertical crack resulted from the cooling of the concrete, and the evaluation of the width of the crack opening resulting from each of the various load combinations was one of the principal objects of the studies. In addition, the stress distribution within the section (particularly in the stress concentration zones at the ends of the crack and at the toe and heel of the dam) as well as its overall displacements were of interest. An uncracked section also was studied so that a comparison of the results for the two systems might demonstrate directly the influence of the crack.

## THE FINITE ELEMENT METHOD

Because the finite element method has been described previously, only a brief description of the general features of the method will be given here. In addition, certain features of the present study which have not been presented before will be discussed in greater detail. In general, the method consists of idealizing the actual continuous system as an assemblage of triangular plate elements, interconnected only at the corners, and also loaded only at these points. Within each element, the normal and shear stresses are assumed uniform, thus continuity between the elements is maintained even though they are connected only at the nodal points.

The analysis involves first calculating the stiffnesses of the individual triangular elements; then by adding together the pertinent element stiffnesses, the stiffness of the assembled system is determined. This assembled structure stiffness is represented by the matrix [K] in the equation:

$$\{R\} = [K]\{r\} \tag{1}$$

where also

$\{R\}$ = vector of all nodal point force components
$\{r\}$ = vector of corresponding nodal point displacements.

This equation can be solved formally for the displacements resulting from specified loads by inverting the stiffness matrix. However, in the present study, this matrix was too large to be inverted conveniently, and the displacements were determined from Eq. (1) by an iteration process.

After the nodal point displacements have been obtained, the stress components in each of the triangular elements (which are linearly related to the displacements) can be obtained by the matrix multiplication:

$$\{\sigma\} = [M]\{r\} \tag{2}$$

in which

$\{\sigma\}$ = vector of all element stresses $\sigma_x$, $\sigma_y$, $\tau_{xy}$
$[M]$ = stress transformation matrix.

In this study, the principal stresses in the elements and their directions were also determined, in addition to the $x$, $y$ stresses.

### Element Idealizations

The finite element idealizations used in this study are shown in figure 2. The coarse mesh idealization in figure 2*a* was used in preliminary analyses in order to determine the displacements at the base of the foundation system used in the fine mesh analysis (shown by the dashed line). Thus it was possible to retain the effect of a deep foundation in the fine mesh idealization shown in figure 2*b* without devoting a large number of elements to the foundation zone. It was necessary, of course, to make a separate coarse mesh analysis for each of the loading conditions which were applied to the fine mesh system. In the coarse mesh system, there are a total of 103 elements and 69 nodal points, while in the fine mesh system the numbers are 194 and 130 respectively.

### Element Stiffness

The derivation of the stiffness matrix of an arbitrary isotropic plane stress element is presented in [1], and will not be repeated here. It is of interest to note, however, that this same stiffness matrix can be applied in a plane strain analysis if modified material properties are used, as follows:

$$E^* = \frac{E}{1-\nu^2} \qquad \nu^* = \frac{\nu}{1-\nu} \tag{3}$$

where $E$ = modulus of elasticity (actual)
$\nu$ = Poissons' ratio (actual)

and the starred values represent the modified properties to be used in a plane strain analysis. The plane stress condition was considered to be more applicable in the present study; but with the assumed value of Poisson's ratio, the difference between the two conditions is negligible: $E^*/E = 1.03$, $\nu^*/\nu = 1.20$.

In order to represent the orthotropic foundation material, it was necessary to develop an orthotropic element stiffness matrix. For this purpose, the stress-strain relationship for an orthotropic material was needed. In this derivation, it was assumed that the orthotropic material actually consisted of a horizontally layered system of alternately hard and soft isotropic materials. Designating the properties of these materials $E_1$, $\nu_1$ and $E_2$, $\nu_2$ respectively, it was further assumed that:

$$\frac{E_1}{\nu_1} = \frac{E_2}{\nu_2}. \tag{4}$$

On the basis of these assumptions, the orthotropic stress-strain relationship was found to be

$$\begin{bmatrix} \varepsilon_x \\ \varepsilon_y \\ \gamma_{xy} \end{bmatrix} = \frac{1}{E_x} \begin{bmatrix} 1 & -\nu_x & 0 \\ -\nu_x & \mu & 0 \\ 0 & 0 & 2(\mu + \nu_x) \end{bmatrix} \tag{5}$$

in which

$$E_x = E_1 (1 - r^*); \; r^* = r\left(1 - \frac{E_2}{E_1}\right)$$

$$\nu_x = \nu_1 (1 - r^*)$$

$$\mu = \frac{E_x}{E_y}; \; E_y = \frac{E_2}{r^* + \frac{E_2}{E_1}}$$

and $r$ is the proportion of the total volume occupied by the soft layers. Using this orthotropic stress-strain law, the derivation of the orthotropic element stiffness followed exactly the procedure described in [1] for the isotropic triangular element stiffness.

### Loadings

The load vector $\{R\}$ in Eq. (1) is merely a listing of all the load components applied at the nodal points in any given analysis. For each nodal point, the dead load force was computed by taking one-third of the total weight of all elements attached to the nodal point. Live load (water) forces were applied only at the nodal points in contact with the water, of course, and were taken as the concentrated static equivalent of the distributed water pressures acting on these elements.

The thermal loads were calculated by first determining the stresses which would exist if all strains due to temperature changes were constrained. In a plane stress system, these stresses are given by

$$\sigma = -\frac{E\alpha}{1 - \nu} \Delta T \qquad (6)$$

in which $\alpha$ = thermal coefficient of expansion
$\Delta T$ = change of temperature.

The nodal forces required to maintain these stresses in each element were then found by simple statics. Finally, since these nodal constraints did not really exist, their effect was eliminated by applying equal and opposite nodal forces.

These *reversed* nodal forces are the thermal loads for which the section was analyzed. Displacements resulting from these effective loads are the true thermal displacements in the system. The total thermal stresses were determined by combining the constrained stress of Eq. (6) with the stresses resulting from these thermal loads.

## THE DIGITAL COMPUTER PROGRAM

Practical applications of the finite element method described above require such a tremendous amount of computational effort that they may be performed only by means of automatic digital computers. A special program designed to perform such analyses for arbitrary finite element idealizations has been written for the IBM 704 operated by the University of California Computer Center, and was used in all of the work described in this report.

The computer program performs three major tasks in the complete analysis of a plane stress system. First, the element stiffness and load matrices are formed from a basic numerical description of the structure. Second, Eq. (1) is solved for the displacements of the nodal points by an iteration procedure. Third, the internal element stresses are determined from these displacements. Only the main operations of the computer program will be described here; details of the coding will be omitted. The operation of the program is flexible in that both input and output can be « on-line » or may be effected « off-line » through the use of magnetic tapes and peripheral equipment.

### Numerical Procedure

Before presenting the sequence of operations that is performed by the computer program, it is necessary to discuss in some detail the actual numerical procedure that was employed. This method is a modification of the well-known Gauss-Seidel iteration procedure which, when applied to Eq. (1), involves the repeated calculation of new displacements from the equation

$$r_n^{(s+1)} = (k_{nn})^{-1} \left[R_n - \sum_{i=1,n-1} k_{ni} r_i^{(s+1)} - \sum_{i=n+1,N} k_{ni} r_i^{(s)}\right] \qquad (7)$$

where $n$ = number of the displacement component
$s$ = cycle of iteration

The only modification of the procedure introduced in this analysis is the application of Eq. (7) simultaneously to both components of the displacement at each nodal point. Therefore $r_n$ and $R_n$ become vectors with $x$ and $y$ components, and the stiffness coefficients are in the form

$$k_{lm} = \begin{bmatrix} k_{xx} & k_{xy} \\ k_{yx} & k_{yy} \end{bmatrix}_{lm} \qquad (8)$$

in which $l$ and $m$ are nodal point numbers.

### Over-Relaxation Factor

The rate of convergence of the Gauss-Seidel procedure can be greatly increased by the use of an over-relaxation factor [3]. However, in order to apply this factor it is first necessary to calculate the change in the displacement of nodal point $n$ between cycles of iteration:

$$\Delta r_n^{(s)} = r_n^{(s+1)} - r_n^{(s)}. \qquad (9)$$

The substitution of Eq. (7) into Eq. (9) yields for the change in displacement

$$\Delta r_n^{(s)} = (k_{nn})^{-1} \left[R_n - \sum_{i=1,n-1} k_{ni} r_i^{(s+1)} - \sum_{i=n,N} k_{ni} r_i^{(s)}\right] \qquad (10)$$

The new displacement of nodal point $n$ is then determined from the following equation:

$$r^{(s+1)} = r_{nn}^{(s)} + \beta \Delta r_n^{(s)} \qquad (11)$$

where $\beta$ is the over-relaxation factor. For the structure considered in this report it was found that a value of $\beta$ equal to 1.86 gave the most rapid convergence.

### Physical Interpretation of Method

Important physical significance can be attached to the terms of Eq. (10). The term $(k_{nn})^{-1}$ is the flexibility of nodal point $n$. This represents the nodal point displacements resulting from unit nodal point forces, and can be written in the form of a sub-matrix:

$$(k_{nn})^{-1} = \begin{bmatrix} f_{xx} & f_{xy} \\ f_{yx} & f_{yy} \end{bmatrix}_n . \qquad (12)$$

The summation terms represent the elastic forces acting at nodal point $n$ due to the deformations of the plate elements:

$$Q_n^{(s+1)} = \sum_{i=1,n-1} k_{ni} r_i^{(s+1)} + \sum_{i=n,N} k_{ni} r_i^{(s)} . \qquad (13)$$

The difference between these elastic forces and the applied loads is the total unbalanced force, which in sub-matrix form may be written:

$$\begin{Bmatrix} X \\ Y \end{Bmatrix}_n^{(s+1)} = \begin{Bmatrix} R_x \\ R_y \end{Bmatrix}_n - \begin{Bmatrix} Q_x \\ Q_y \end{Bmatrix}_n^{(s+1)} . \qquad (14)$$

Equation (11) which gives the new displacement of nodal point $n$, may now be written in the following sub-matrix form:

$$\begin{Bmatrix} r_x \\ r_y \end{Bmatrix}_n^{(s+1)} = \begin{Bmatrix} r_x \\ r_y \end{Bmatrix}_n^{(s)} + \beta \begin{bmatrix} f_{xx} & f_{xy} \\ f_{yx} & f_{yy} \end{bmatrix}_n \begin{Bmatrix} X \\ Y \end{Bmatrix}_n^{(s+1)} . \qquad (15)$$

It is important to note that any desired nodal point displacement may be assumed for the first cycle of iteration. A good choice of these displacements will greatly speed the convergence of the solution. In fact, if all displacements were assumed correctly, the unbalanced forces given by Eq. (14) would be zero, and no iteration would be necessary. However, in a practical case, there always will be unbalanced forces in the system at first, and the iteration process continually reduces them toward zero.

### Input Data

For the purpose of defining the structure, all nodal points and elements are numbered, consecutively. The numerical description is read into the machine in the form of punched cards, by the following four arrays:

A. Parameter Array (6 numbers):
1. Number of elements.
2. Number of nodal points.
3. Number of boundary points.
4. Over-relaxation factor $\beta$.
5. Convergence limit.
6. Coefficient of thermal expansion $\alpha$.

B. Element Array (9 numbers per element):
1. Element number.
2. Number of nodal point *i*.
3. Number of nodal point *j*.
4. Number of nodal point *k*.
5. Modulus of elasticity E
6. Poisson's ratio $\upsilon$
7. Unit weight of element $\gamma$
8. Temperature change within element $\Delta T$
9. Orthotropic factor $\mu = \frac{E_x}{E_y}$

C. Nodal Point Array (7 numbers per nodal point):
1. Nodal point number.
2. x-ordinate.
3. y-ordinate,
4. x-load.
5. y-load.
6. Initial x-displacement.
7. Initial y-displacement.

D. Boundary Condition (2 numbers per boundary point):
1. Nodal point number.
2. This number indicates the type of constraint: « O » for a point fixed both vertically and horizontally, the only boundary constraint condition considered in this investigation.

### Output Information

At specified intervals in the iteration procedure, nodal displacements and element stresses are printed. Figure 3 illustrates the form of the computer output in a typical case. In addition, the sum of the absolute magnitude of the unbalanced forces at all nodal points (Eq. 14), which is computed for each cycle, is printed out as a check on the convergence of the procedure. In all analyses made during the course of this investigation, this sum was reduced to less than 1/1000 of its value after the first cycle of iteration.

### Timing

The computational time required by the program is approximately equal to 0.07 n.m seconds, where $n$ equals the number of nodal points and $m$ equals the number of cycles of iteration. The number of cycles required depends on the accuracy of the initially assumed displacements and on the desired degree of convergence. For the structure considered in this report, the computer time per solution was approximately 7 minutes for the coarse mesh and 17 minutes for the fine mesh. The number of cycles of iteration for the various cases ranged from about 70 to 100.

## RESULTS

Although the printed output of the computer, as shown in figure 3, contained the complete results of the investigation, they were also presented graphi-

| ELEMENT | (PSI) X-STRESS | (PSI) Y-STRESS | (PSI) XY-STRESS | (PSI) MAX-STRESS | (PSI) MIN-STRESS | (DEGREES) DIRECTION |
|---|---|---|---|---|---|---|
| 1 | -21.637024 | -40.614304 | 33.432649 | 3.6 | -65.9 | -37.1 |
| 2 | 15.095711 | 3.577621 | 21.158474 | 31.3 | -12.6 | -37.4 |
| 3 | -42.514305 | -38.270859 | 2.591661 | -37.0 | -43.7 | -64.7 |
| 4 | -31.742538 | -16.989304 | 14.911327 | -7.7 | -41.0 | -58.2 |
| 5 | -5.087471 | 9.535896 | -4.226090 | 10.7 | -6.2 | 75.0 |
| 6 | -60.592682 | -21.883614 | 5.673300 | -21.1 | -61.4 | -81.8 |
| 7 | 3.596840 | -6.501434 | 8.060141 | 8.1 | -11.0 | -29.0 |
| 8 | -41.907402 | 8.325272 | 22.115488 | 16.7 | -50.3 | -69.3 |
| 9 | -29.894760 | -14.201363 | 2.760811 | -13.7 | -30.4 | -80.3 |
| 10 | -19.019836 | -113.042328 | 41.108610 | -3.6 | -128.5 | -20.6 |
| 11 | -9.670067 | -3.545715 | 1.172920 | -3.3 | -9.9 | -79.5 |
| 12 | -19.362946 | 24.689590 | 0.280712 | 24.7 | -19.4 | -89.6 |
| 13 | -42.158066 | 2.489532 | -3.621626 | 2.8 | -42.4 | 85.4 |
| 14 | -13.876846 | 9.762047 | -1.376879 | 9.8 | -14.0 | 86.7 |
| 15 | -55.332329 | 12.838753 | 11.194128 | 14.6 | -57.1 | -80.9 |
| 16 | -11.221085 | 21.112564 | 13.384552 | 25.9 | -16.0 | -70.2 |
| 17 | -61.941177 | -16.112938 | 31.179846 | -0.3 | -77.7 | -63.2 |
| 18 | 14.900993 | -10.251991 | 33.216614 | 37.8 | -33.2 | -34.6 |
| 19 | -77.299423 | -18.673866 | 45.481194 | 6.1 | -102.1 | -61.4 |
| 20 | -68.392212 | -25.644630 | 21.986590 | -16.4 | -77.7 | -67.1 |
| 21 | -34.477783 | -10.517090 | 11.790384 | -5.7 | -39.3 | -67.7 |
| 22 | -7.344345 | 8.977432 | -4.832099 | 10.3 | -8.7 | 74.7 |
| 23 | -34.220215 | 23.321732 | -8.167995 | 24.5 | -35.4 | 82.1 |
| 24 | -11.582161 | 32.631912 | -2.718958 | 32.8 | -11.7 | 86.5 |
| 25 | -46.657974 | 19.291512 | 3.835845 | 19.5 | -46.9 | -86.7 |
| 26 | -13.946526 | 43.675842 | 18.032915 | 48.9 | -19.1 | -74.0 |
| 27 | -83.458755 | -12.719467 | 45.440448 | 9.5 | -105.7 | -63.9 |
| 28 | -4.890427 | 13.208176 | 37.164865 | 42.4 | -34.1 | -51.8 |
| 29 | 1.348351 | -10.524033 | 30.664423 | 26.6 | -35.8 | -39.5 |
| 30 | -102.706940 | -89.829132 | 46.319461 | -49.5 | -143.0 | -49.0 |
| 31 | -36.349174 | -70.508469 | 66.600939 | 15.3 | -122.2 | -37.8 |
| 32 | -1.370247 | -44.906326 | 25.714500 | 10.6 | -56.8 | -24.9 |
| 33 | -26.064774 | -64.952545 | 59.050345 | 16.7 | -107.7 | -35.9 |
| 34 | -20.962494 | -16.453156 | 14.811054 | -3.7 | -33.7 | -49.3 |
| 35 | -32.728851 | -5.217323 | 2.676623 | -5.0 | -33.0 | -84.5 |
| 36 | -45.844315 | 15.385841 | -0.936499 | 15.4 | -45.9 | 89.1 |
| 37 | -22.696800 | 12.184837 | -2.723261 | 12.4 | -22.9 | 85.6 |
| 38 | -9.309067 | 33.630989 | -7.344516 | 34.9 | -10.5 | 80.6 |
| 39 | -16.388954 | 38.171394 | -4.737985 | 38.6 | -16.8 | 85.1 |
| 40 | 29.606812 | 46.513466 | 2.932751 | 47.0 | 29.1 | -80.4 |
| 41 | -6.309235 | 29.010864 | -7.292584 | 30.5 | -7.8 | 78.8 |
| 42 | 41.728279 | 65.571236 | 81.198050 | 135.7 | -28.4 | -49.2 |
| 43 | -18.289627 | -15.782555 | 19.939212 | 2.9 | -37.0 | -46.8 |
| 44 | 22.005043 | -23.887611 | 62.266115 | 65.4 | -67.3 | -34.9 |
| 45 | -9.252480 | -55.976212 | 39.016029 | 12.9 | -78.1 | -29.5 |
| 46 | -23.453789 | -69.528412 | 51.371544 | 9.8 | -102.8 | -32.9 |
| 47 | -57.654015 | -19.821014 | 12.165121 | -16.2 | -61.2 | -73.6 |
| 48 | -16.010735 | -1.447845 | 13.872331 | 6.9 | -24.4 | -58.8 |
| 49 | -53.434456 | 6.212318 | 3.402412 | 6.4 | -53.6 | -86.7 |
| 50 | -11.542534 | 29.182938 | 16.814773 | 35.2 | -17.6 | -70.2 |
| 51 | -33.487152 | 19.204918 | 16.218376 | 23.8 | -38.1 | -74.2 |

| NODAL POINT | (INCHES) X-DISPLACEMENT | (INCHES) Y-DISPLACEMENT |
|---|---|---|
| 1 | 0.045173 | -0.029458 |
| 2 | 0.058178 | -0.013816 |
| 3 | 0.130151 | -0.034537 |
| 4 | 0.166736 | -0.067413 |
| 5 | 0.190258 | -0.100647 |
| 6 | 0.209396 | -0.136003 |
| 7 | 0.225354 | -0.171480 |
| 8 | 0.238976 | -0.207627 |
| 9 | 0.250559 | -0.243729 |
| 10 | 0.261115 | -0.279447 |
| 11 | 0.272950 | -0.320961 |
| 12 | 0.289812 | -0.371849 |
| 13 | 0.297384 | -0.398693 |
| 14 | 0.238857 | -0.416963 |
| 15 | 0.237644 | -0.395673 |
| 16 | 0.191532 | -0.400589 |
| 17 | 0.232356 | -0.337109 |
| 18 | 0.190137 | -0.351804 |
| 19 | 0.149180 | -0.364911 |
| 20 | 0.141777 | -0.380089 |
| 21 | 0.129665 | -0.372276 |
| 22 | 0.238763 | -0.288985 |
| 23 | 0.196613 | -0.306839 |
| 24 | 0.154202 | -0.323265 |
| 25 | 0.111614 | -0.336806 |
| 26 | 0.087621 | -0.344180 |
| 27 | 0.201616 | -0.264921 |
| 28 | 0.159523 | -0.282565 |
| 29 | 0.117430 | -0.297379 |
| 30 | 0.096284 | -0.302664 |
| 31 | 0.090143 | -0.324456 |
| 32 | 0.068399 | -0.327413 |
| 33 | 0.070444 | -0.305661 |
| 34 | 0.046395 | -0.305916 |
| 35 | 0.205631 | -0.222702 |
| 36 | 0.163587 | -0.241099 |
| 37 | 0.123230 | -0.257917 |
| 38 | 0.084663 | -0.269945 |
| 39 | 0.071567 | -0.268477 |
| 40 | 0.048155 | -0.267604 |
| 41 | 0.016155 | -0.265461 |
| 42 | 0.207651 | -0.180322 |
| 43 | 0.164601 | -0.199870 |
| 44 | 0.122949 | -0.217015 |
| 45 | 0.083207 | -0.233610 |

FIG. 3. — **Digital computer output.**

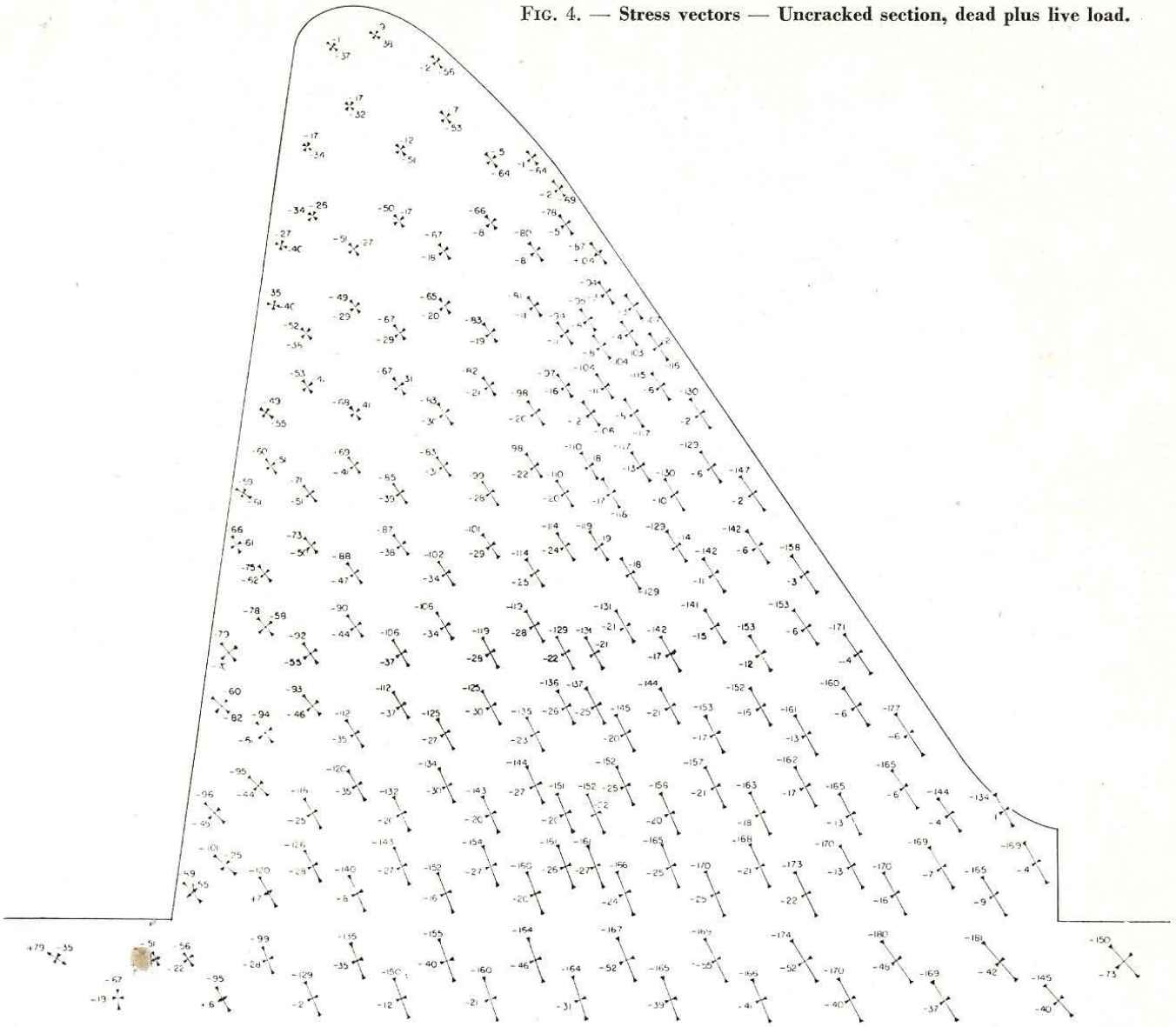

FIG. 4. — **Stress vectors — Uncracked section, dead plus live load.**

cally in order that they might be more easily interpreted. Stress results were presented in two types of charts. Stress Vectors, shown in figure 4 for the dead plus live load acting on the uncracked section, are merely a direct graphical representation of the magnitudes and directions of the principal stresses, plotted from the center of each element. Such figures give a good qualitative picture of the state of stress in the section; but for quantitative studies, the Stress Contours, shown in figures 5, 6, and 7 are preferable. These contours, or iso-static lines, are lines of constant stress on the section. They clearly indicate the areas of high stress concentration.

Although it is not the purpose of this paper to discuss the specific results obtained in the investigation, a few comments with regard to these figures may be of interest. Figure 5 shows the stress distribution in the section with a crack extending through 7/9 of the height, when subjected to dead plus live loads. The compressive stress concentrations at the base and top of the crack, and the tensile stress zones at the heel and near the top of the crack are of particular interest here. A comparison of the two cases shown in figure 6 demonstrates the importance of the temperature stresses on the uncracked section, in comparison with those due to dead plus live loading. Comparison of figure 7 with figure 5a indicates the relatively small influence exerted by the reduced vertical modulus of the orthotropic foundation.

Nodal displacement results were also presented in two types of charts. Figure 8 shows the boundary nodal point displacement vectors. Lines connecting the ends of these vectors show the outline of the deformed structure, to an exaggerated scale. Of more interest in this investigation, however, was the

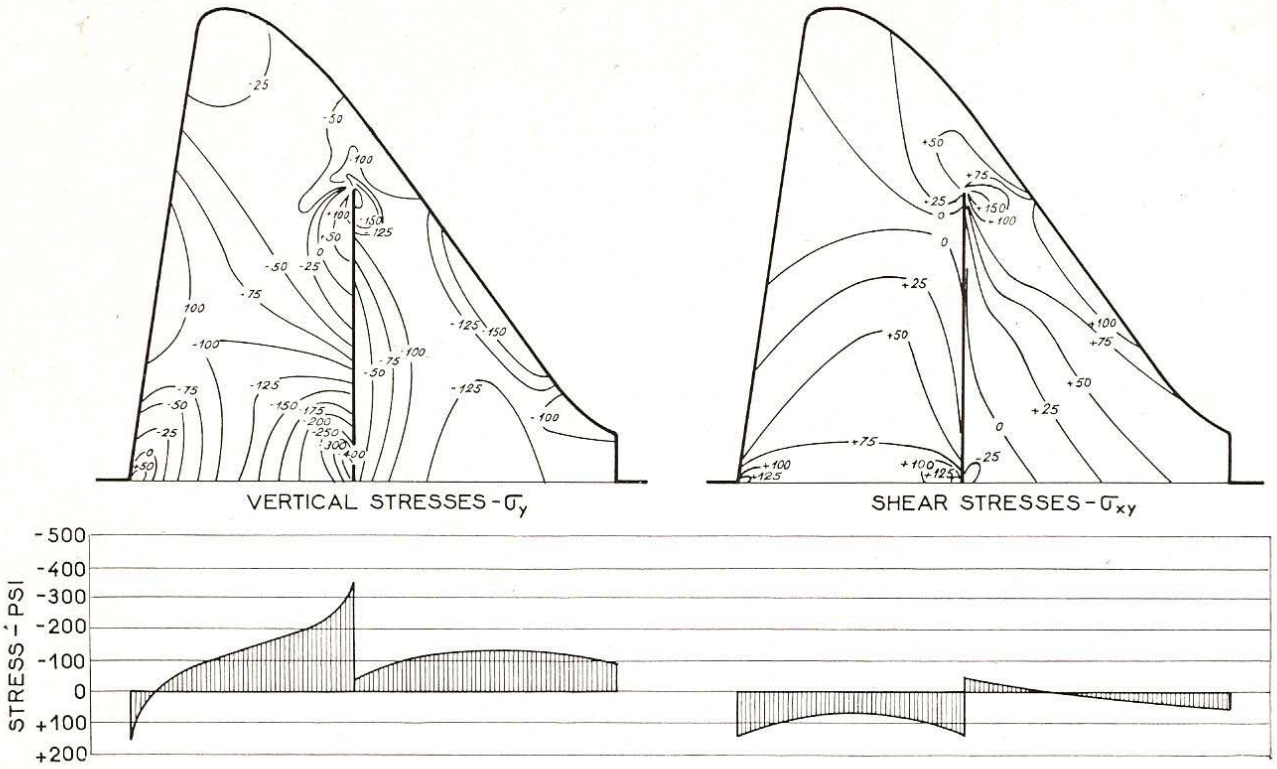


FIG. 5. — **Stress contours — 7/9 crack height, dead plus live load.**

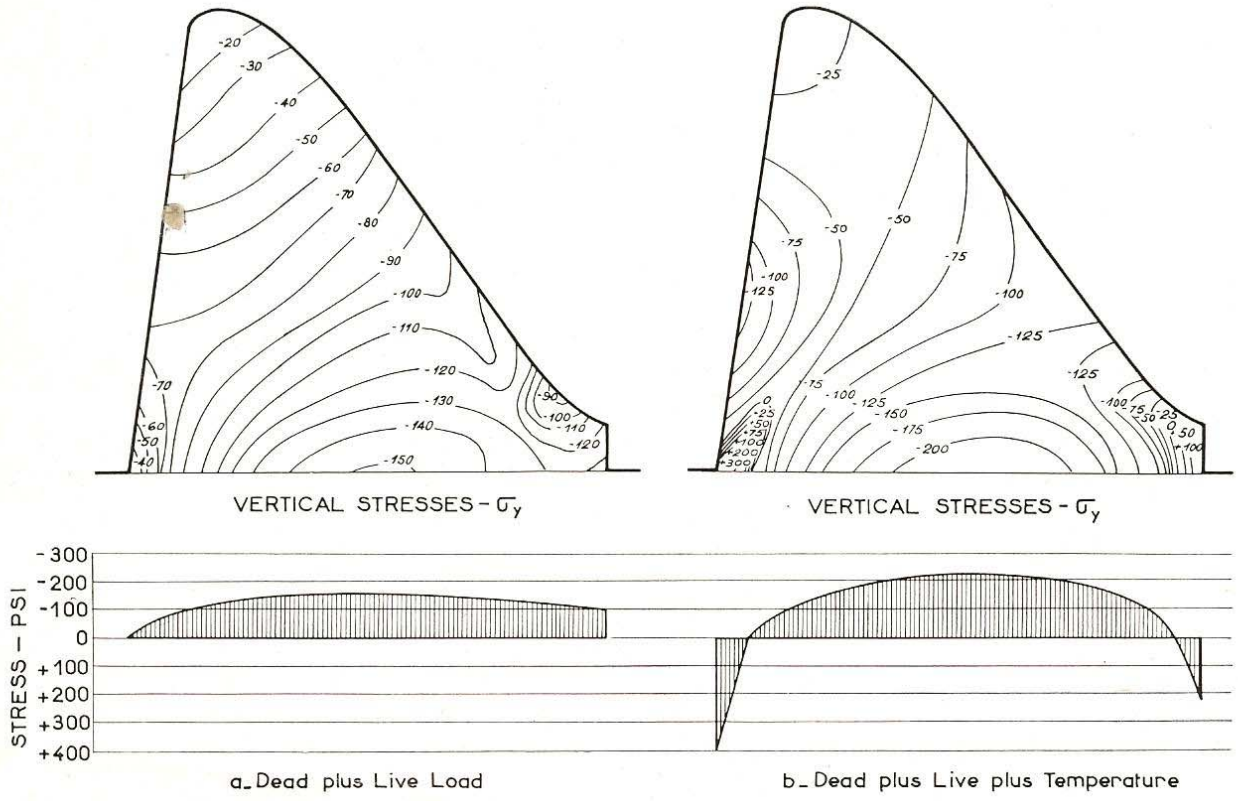


FIG. 6. — **Influence of temperature on normal stress distribution — uncracked section.**

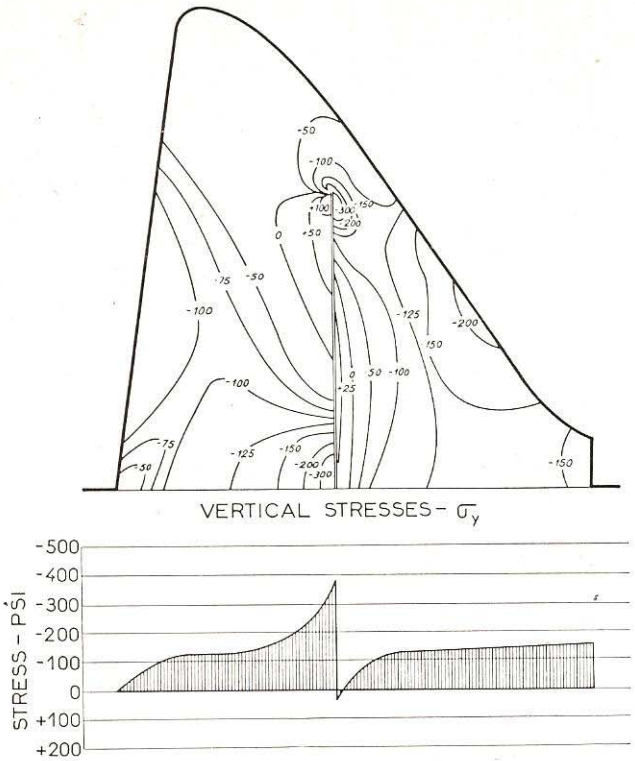


FIG. 7. — **Normal stress distribution with orthotropic foundation — 7/9 crack height— dead plus live load.**

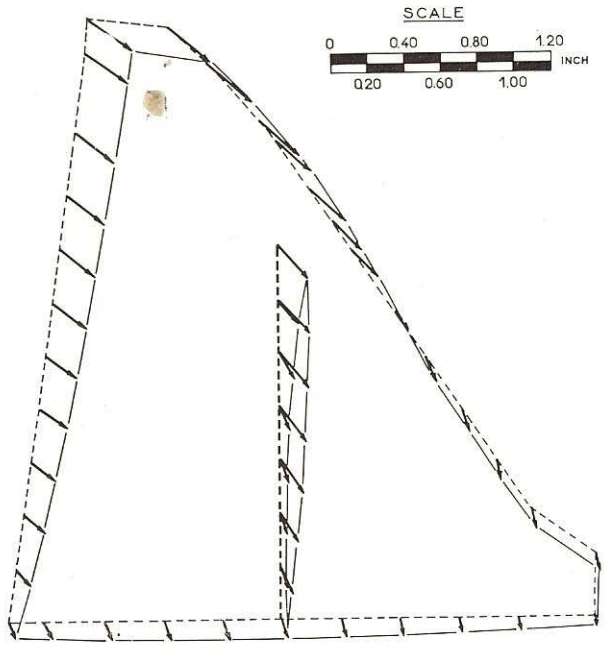


FIG. 8. — **Boundary displacements — 7/9 crack height, dead plus live load.**

relative displacement of the two sides of the crack, shown in figure 9. Here the successive effects of temperature, dead load, and dead plus live load on the crack opening are clearly indicated. It is of interest to note that the live loading was not sufficient to close the crack completely.

## CONCLUSIONS

This investigation has clearly demonstrated the applicability and practicality of the finite element method in solving large-scale and complex plane stress (or plane strain) elasticity problems. One of the most important attributes of the method is its versatility, which results from its discrete (rather than continuous) representation of the system. Because each element is treated individually, it may be assigned properties completely without regard for the properties of its neighbours. Thus, the difference between the moduli of the foundation rock and the concrete of the dam, and the fact that one material might be orthotropic while the other was isotropic, caused no difficulty whatsoever. Similarly, because the temperature changes were assigned element by element, any desired thermal gradient could be represented.

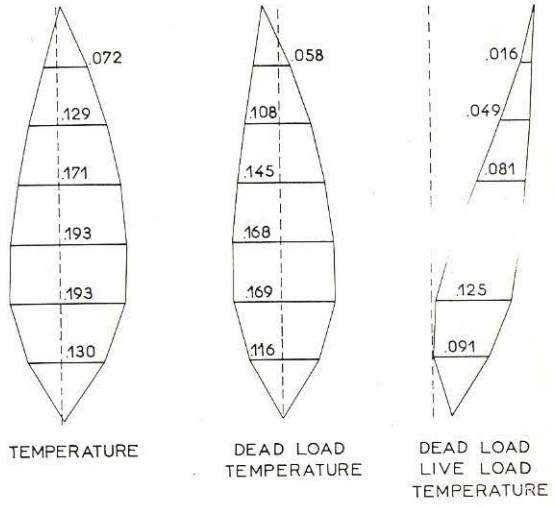


FIG. 9. — **Crack openings — 7/9 crack height.**

Also to be noted is the ease with which the triangular element system can be arranged to fit any specified boundary condition. The internal crack becomes merely another external boundary, by this procedure, and leads to no special problems. Another advantage of the triangular element representation is the fact that different sizes of elements can be employed in different parts of the system during a single analysis. Thus, it is possible to employ small elements in regions of stress concentration and high

stress gradients, while larger elements may be used in areas where the stresses are relatively constant.

The principal disadvantage of the finite element method also results directly from the discrete nature of the idealization. Because the stresses are assumed constant within each element, the discontinuous stress distribution which is computed must be smoothed out graphically to give a better indication of the actual continuous distribution. In the construction of the stress contours in this study, it was assumed that the calculated element stress applied to the center of the element, and the contour lines were located accordingly. Increasing the number of elements tends to reduce the stress discontinuities, of course, but because the computation time increases rapidly with the number of elements, it is desirable to do a certain amount of smoothing graphically.

**ACKNOWLEDGMENT**

Work described in this report was carried out under a University of California, Institute of Engineering Research Contract for the Little Rock District, U. S. Army Corps of Engineers. The authors particularly wish to thank Mr. E. F. Rutt, Chief of the Engineering Division of the Little Rock District, and the Board of Consultants to the District: Dr. R. W. Carlson, Professor R. E. Davis, and Mr. B. W. Steele, for their advice during the course of the investigation.

In addition, Mr. Ian King, graduate student at the University of California, is thanked for the very great part he played in the digital computer analyses. The support of the National Science Foundation, whose research grant made possible the original development of the computer program used in these analyses, is also gratefully acknowledged.

**REFERENCES**

[1] CLOUGH, R. W. — "The Finite Element Method in Plane Stress Analysis", *Proceedings*, Second Conference on Electronic Computation, ASCE Structural Division, Pittsburgh, Pennsylvania, September 1960, p. 345.

[2] CLOUGH, R. W. — "The Stress Distribution of Norfork Dam", University of California, *Institute of Engineering Research Report*, Series 100, Issue No. 19, March 1962.

[3] LEHMANN, F. G. — "Simultaneous Equations Solved by Over-Relaxation", *Proceedings*, Second Conference on Electronic Computation, ASCE Structural Division, Pittsburgh, Pennsylvania, September 1960, p. 503.

## *Historical remarks by Ed Wilson - 2013*

At the time Ray wrote this 12 page paper he had approved the final draft of my Doctor of Engineering Dissertation which was later published as a 72 page report "Finite Element Analysis of Two Dimensional Structures", UCB/SESM Report No. 63/2, University of California Berkeley, June 1963. The analysis of Norfork Dam was included as an example, in addition to other examples. The dissertation also included improvements to the Gauss-Seidel iteration method and extension of the FEM to the analysis of structures with nonlinear materials. However, the major reason copies of my dissertation were requested by thousands of structural engineers was to obtain the Appendix, which contained the six page users' manual and the ***six page*** FORTRAN listing of the linearly elastic version of the FEM program. A few years later, an engineer in Washington modified the program and sold it for $30,000.

The policy of freely distributing the structural engineering software, which was developed by graduate students and me, continued for the next 22 years. During this period of time, my research was motivated and funded by my consulting work and solving real engineering problems. In addition, Professor Jack Bouwkamp and I had a small ongoing NSF project for the dynamic field testing of structures and comparing results with computer program predictions. In 1984 our proposal to continue the project was rejected by NSF and it was necessary to personally fund one graduate student. It was at that point in time; I decided structural analysis programs, developed (in FORTRAN) on my personal computer at home, would no longer be freely given away. It was a great opportunity to develop a new generation of structural engineering software to operate on inexpensive personal computers. Looking back, the loss of the NSF project funding was one of the best days of my life. Also, I will always be thankful to Ray Clough for placing my name on this historic paper.

Sequence of Operations

Input Data - For the purpose of numerically defining a structure, all nodal points and elements are numbered as illustrated in Fig. 16. The following sequence of punched cards numerically defines the structure.

A. Title Card (72H)
Columns 2 to 72 of this card contain information to be printed with result.

B. Control Card (6I4, 2E12.5, 1I1)

| Cols. | | |
|---|---|---|
| | 1-4 | Number of elements |
| | 5-8 | Number of nodal points |
| | 9-12 | Number of restrained boundary points |
| | 13-16 | Cycle interval for the print of the force unbalance |
| | 17-20 | Cycle interval for the print of displacements and stresses |
| | 21-24 | Maximum number of cycles problem may run |
| | 25-36 | Convergence limit for unbalanced forces |
| | 37-48 | Over-relaxation factor |
| | 49 | Non-zero punch to suppress printing of input data |

C. Element array - 1 card per element (4I4, 4E12.4, F8.4)

| Cols. | | |
|---|---|---|
| | 1-4 | Element number |
| | 5-8 | Nodal point number i |
| | 9-12 | Nodal point number j |
| | 13-16 | Nodal point number k |
| | 17-28 | Modulus of elasticity |
| | 29-40 | Density of element |
| | 41-52 | Poisson's Ratio |
| | 53-64 | Coefficient of thermal expansion |
| | 65-72 | Temperature change within element |

D. Nodal point array - 1 card per nodal point (1I4, 4F8.1, 2F12.8)

| Cols. | | |
|---|---|---|
| | 1-4 | Nodal point number |
| | 5-12 | X-ordinate |
| | 13-20 | Y-ordinate |
| | 21-28 | X-load |
| | 29-36 | Y-load |
| | 37-48 | X-displacement } on free nodal points, these are initial guesses, on |
| | 49-60 | Y-displacement } restrained nodal points, these are specified displacements. |

E. Boundary array - 1 card per point (2I4,IF6)

| Cols. | | |
|---|---|---|
| | 1-4 | Nodal point number |
| | 5-8 | 0 if Nodal point is fixed in both directions<br>1 if Nodal point is fixed in X-direction.<br>2 if Nodal point is free to move along a line of slope S. |
| | 9-16 | Slope S (type 2 boundary point only) |

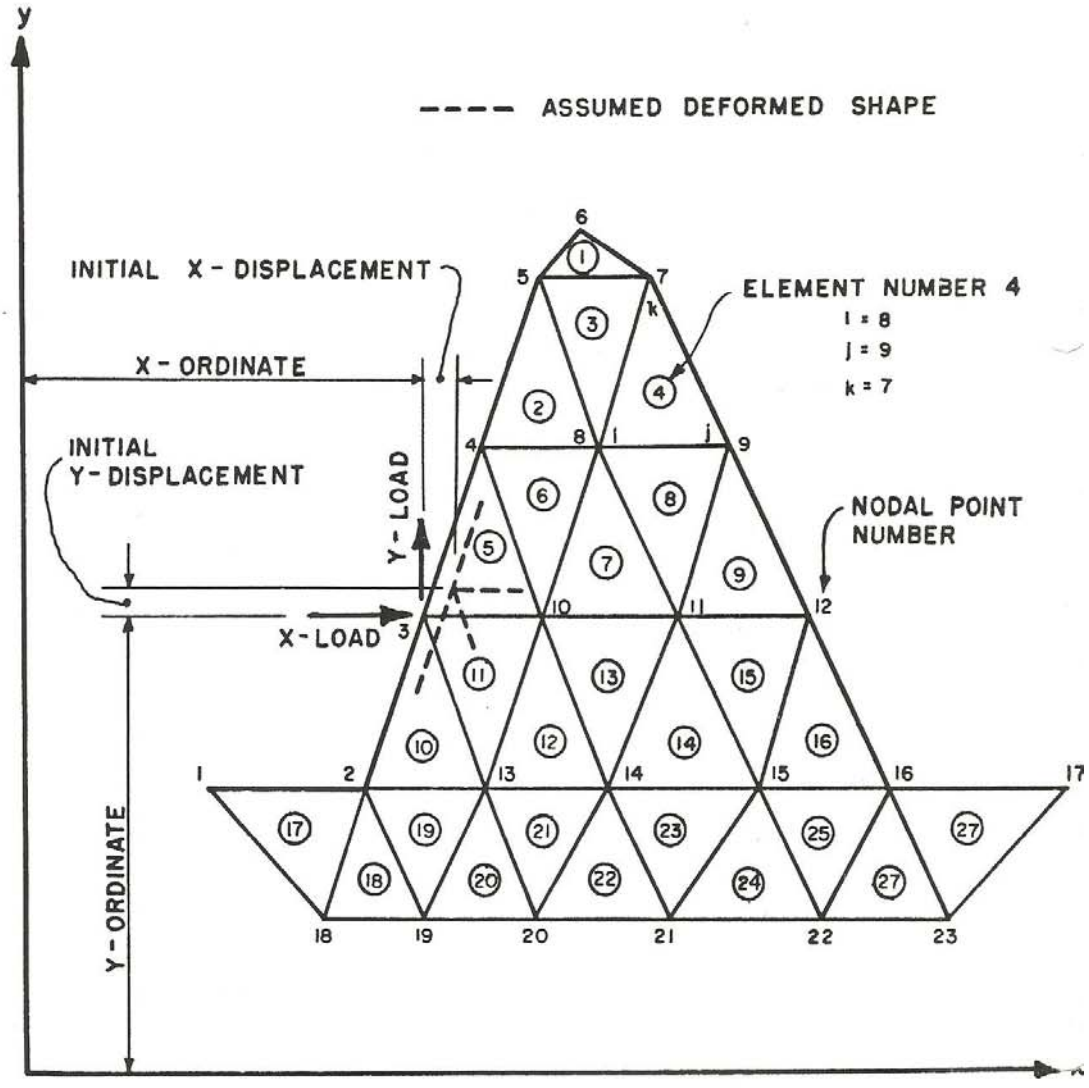


FIG. 16 NUMBERING SYSTEM FOR ELEMENTS AND NODAL POINTS

It should be noted that for a fixed boundary point, the initial displacement is the final displacement of the point, since it is not altered by the iteration procedure.

Formation of Element Stiffness Matrices - The stiffness matrix for each element is determined from Eq. 11. The basic element dimensions are calculated from the coordinates of the connecting nodal points:

$$a_j = X_j - X_i$$
$$b_j = Y_j - Y_i$$
$$a_k = X_k - X_i$$
$$b_k = Y_k - Y_i$$

where i, j and k are the nodal point numbers of the three connecting points and are given in the element array.

Formation of Complete Stiffness of System - Because of the large matrices that are developed in the solution of practical problems, the stiffness matrix used in Eq. 12 is not formed. Since the complete stiffness matrix contains many zero elements, only the non-zero elements are developed and retained by the program; thus, it is possible to treat large plane stress systems without exceeding the storage capacity of the computer.

Formation of Nodal Point Loads - The loads acting on the nodal points are composed of live loads, dead loads, and temperature loads. The equations which are used to determine these loads have been presented in the preceding sections of this report.

Formation of Nodal Flexibilities - The nodal point flexibilities are determined from the previously developed stiffness coefficients. The flexibilities associated with the boundary nodal points are modified by the application of Eqs. 30, as required.

Iterative Solution - The repeated application of Eq. 27 at all nodal points constitutes the iterative procedure. The sum of the absolute magnitude of the unbalanced forces at all nodal points (given by Eq. 26) is also computed for each cycle; this sum, when compared to the covergence limit, serves as a check on the convergence of the procedure. In all analyses presented in this report, this sum was reduced to less than 1/10000 of the value obtained in the first cycle of iteration.

Calculation of Stresses - From the nodal point displacements, with the aid of Eq. 8 and Eq. 33, the stresses $\sigma_x$, $\sigma_y$, and $\tau_{xy}$ are calculated for all element and nodal points. As added information, the principal stresses $\sigma_1$ and $\sigma_2$ and directions $\theta$ are also calculated.

Output Information - At desired points in the iteration procedure, nodal displacements, element stresses and nodal point stresses are printed. Fig. 17 illustrates the form of the computer output, in a typical case.

Timing

For the IBM 7090 the computational time required by the program is approximately equal to 0.006 n.m seconds, where n equals the number of nodal points and m equals the number of cycles of iteration. The number of cycles required depends on the accuracy of the initially assumed displacements and on the desired degree of convergence.

| NODAL POINT | X-DISPLACEMENT | Y-DISPLACEMENT |
|---|---|---|
| 1 | 0.889282E-02 | C.885282E-03 |
| 2 | 0.9C1966E-02 | -C.901966E-03 |
| 3 | 0.780701E-02 | -C.78C7C1E-03 |
| 4 | 0.710852E-02 | C.71C852E-03 |
| 5 | 0.653899E-02 | -C.653899E-03 |
| 6 | 0.590251E-02 | C.59C251E-03 |
| 7 | 0.557266E-02 | -C.557266E-03 |
| 8 | 0.516712E-02 | C.516712E-03 |
| 9 | 0.486274E-02 | -C.486274E-03 |
| 10 | 0.455815E-02 | C.455815E-03 |
| 11 | 0.439421E-02 | -C.439421E-03 |
| 12 | 0.421725E-02 | C.421725E-03 |
| 13 | 0.4C7061E-02 | C.407061E-03 |
| 14 | 0.4C6246E-02 | C.262212E-04 |
| 15 | 0.4C7286E-02 | -C.407286E-03 |

| N-POINT | X-STRESS | Y-STRESS | XY-STRESS | MAX-STRESS | MIN-STRESS | DIRECTION |
|---|---|---|---|---|---|---|
| 1 | -1.5910 | 2.8814 | 0.C177 | 2.88 | -1.99 | -89.79 |
| 2 | -2.28C0 | 3.1106 | 0.1642 | 3.12 | -2.29 | -88.26 |
| 3 | -1.8382 | 2.4179 | 0.C536 | 2.42 | -1.84 | -89.28 |
| 4 | -1.4487 | 1.9338 | -0.C289 | 1.93 | -1.45 | 89.51 |
| 5 | -1.1172 | 1.6183 | 0.C399 | 1.62 | -1.12 | -89.17 |
| 6 | -0.8312 | 1.3193 | -0.C255 | 1.32 | -0.83 | 89.32 |
| 7 | -0.6460 | 1.1353 | 0.C191 | 1.14 | -0.65 | -89.39 |
| 8 | -0.4502 | 0.9763 | -0.C204 | 0.98 | -0.45 | 89.18 |
| 9 | -0.3436 | 0.8389 | 0.C145 | 0.84 | -0.34 | -89.30 |
| 10 | -0.2248 | 0.7219 | -0.C134 | 0.72 | -0.23 | 89.19 |
| 11 | -0.1031 | 0.6400 | 0.C064 | 0.64 | -0.10 | -89.51 |
| 12 | -0.C709 | 0.5920 | -0.C177 | 0.59 | -0.07 | 88.47 |
| 13 | -0.C331 | 0.4581 | -0.C205 | 0.46 | -0.03 | 87.61 |
| 14 | -0.C421 | 0.4853 | 0.C013 | 0.49 | -0.04 | -89.86 |
| 15 | -0.C655 | 0.5145 | 0.C239 | 0.52 | -0.07 | -87.65 |

| ELEMENT | X-STRESS | Y-STRESS | XY-STRESS | MAX-STRESS | MIN-STRESS | DIRECTION |
|---|---|---|---|---|---|---|
| 1 | -2.28C0 | 3.1106 | 0.1642 | 3.12 | -2.29 | -88.26 |
| 2 | -1.8765 | 2.3062 | -0.1289 | 2.31 | -1.88 | 88.24 |
| 3 | -1.4384 | 1.8954 | 0.1256 | 1.90 | -1.44 | -87.85 |
| 4 | -1.0554 | 1.6169 | -0.C833 | 1.62 | -1.06 | 88.22 |
| 5 | -0.8491 | 1.2704 | 0.C773 | 1.27 | -0.85 | -87.91 |
| 6 | -0.6017 | 1.1397 | -0.C704 | 1.14 | -0.60 | 87.69 |
| 7 | -0.4764 | 0.9552 | 0.C504 | 0.96 | -0.48 | -87.98 |
| 8 | -0.3169 | 0.8366 | -0.C412 | 0.84 | -0.32 | 87.95 |
| 9 | -0.2282 | 0.7057 | 0.C343 | 0.71 | -0.23 | -87.90 |
| 10 | -0.1325 | 0.6443 | -0.C333 | 0.65 | -0.13 | 87.55 |
| 11 | -0.C331 | 0.6016 | 0.C006 | 0.60 | -0.03 | -89.94 |
| 12 | -0.C655 | 0.5145 | 0.C239 | 0.52 | -0.07 | -87.65 |
| 13 | -0.C331 | 0.4581 | -0.C205 | 0.46 | -0.03 | 87.61 |



Program Listing - For the sake of completeness, a Fortran listing of the basic computer program for linear analysis is included. This will enable others who may wish to utilize this approach to avoid some of the tedious details of programming. It also should be pointed out that the portions of the program which are associated with the formation and solution of the stiffness matrix are independent of the type of structure and therefore may be used for other problems in structural analysis.

PROGRAM LISTING

```
C       PLANE STRESS ITERATION--JUNE 1962
C
C       DIMENSION AND COMMON STATEMENTS
C
        DIMENSION NPNUM(340),XORD(340),YORD(340),
       1DSX(340),DSY(340),XLOAD(340),YLOAD(340),NP(340,10),SXX(340,9),
       2SXY(340,9),SYX(340,9),SYY(340,9),NAP(340)
        DIMENSION NUME(550),NPI(550),NPJ(550),NPK(550),ET(550),XU(550),
       1RO(550),COED(550),DT(550),THERM(550),AJ(550),BJ(550),AK(550),
       2BK(550),SIGXX(550),SIGYY(550),SIGXY(550),SLOPE(340)
        DIMENSION NPB(340),NFIX(340),LM(3),A(6,6),B(6,6),S(6,6)
        COMMON SXX,SXY,SYX,SYY
        EQUIVALENCE (SIGXX,RO,NPB), (SIGYY,COED,NFIX), (SIGXY,DT,SLOPE)
C
C       READ AND PRINT OF DATA
C
  150   READ 100
        PRINT 99
        PRINT 100
        READ 1, NUMEL,NUMNP,NUMBC,NCPIN,NOPIN,NCYCM,TOLER,XFAC,T1
        PRINT 101,NUMEL
        PRINT 102,NUMNP
        PRINT 103,NUMBC
        PRINT 104,NCPIN
        PRINT 105,NOPIN
        PRINT 106,NCYCM
        PRINT 107,TOLER
        PRINT 108,XFAC
        READ 2,(NUME(N),NPI(N),NPJ(N),NPK(N),ET(N),RO(N), XU(N),COED(N),
       1DT(N),N=1,NUMEL)
        READ 3,(NPNUM(M),XORD(M),YORD(M),XLOAD(M),YLOAD(M),
       1DSX(M),DSY(M),M=1,NUMNP)
        IF (T1) 160,155,160
  155   PRINT 110
        PRINT 2,(NUME(N),NPI(N),NPJ(N),NPK(N),ET(N),RO(N),XU(N),COED(N),
       1DT(N),N=1,NUMEL)
        PRINT 111
        PRINT 109,(NPNUM(M),XORD(M),YORD(M),XLOAD(M),YLOAD(M),
       1DSX(M),DSY(M),M=1,NUMNP)
C
C       INITIALIZATION
C
  160   NCYCLE=0
        NUMPT=NCPIN
        NUMOPT=NOPIN
        DO 175 L=1,NUMNP
        DO 170 M=1,9
        SXX(L,M)=0.0
        SXY(L,M)=0.0
        SYX(L,M)=0.0
        SYY(L,M)=0.0
  170   NP(L,M)=0
        NP(L,10)=0
  175   NP(L,1)=L
```

```
C
C       MODIFICATION OF LOADS AND ELEMENT DIMENSIONS
C
        DO 180 N=1,NUMEL
        ET(N)=ABSF(ET(N))
        I=NPI(N)
        J=NPJ(N)
        K=NPK(N)
        AJ(N)=XORD(J)-XORD(I)
        AK(N)=XORD(K)-XORD(I)
        BJ(N)=YORD(J)-YORD(I)
        BK(N)=YORD(K)-YORD(I)
  176   AREA=(AJ(N)*BK(N)-BJ(N)*AK(N))/2.
        IF (AREA) 701,701,177
  177   THERM(N)=ET(N)*COED(N)*DT(N)/(XU(N)-1.)
        DL=AREA*RO(N)/3.
        XLOAD(I)=THERM(N)*(BK(N)-BJ(N))/2.+XLOAD(I)
        XLOAD(J)=-THERM(N)*BK(N)/2.+XLOAD(J)
        XLOAD(K)=THERM(N)*BJ(N)/2.+XLOAD(K)
        YLOAD(I)=THERM(N)*(AJ(N)-AK(N))/2.+YLOAD(I)-DL
        YLOAD(J)=THERM(N)*AK(N)/2.+YLOAD(J)-DL
  180   YLOAD(K)=-THERM(N)*AJ(N)/2.+YLOAD(K)-DL
C
C       FORMATION OF STIFFNESS ARRAY
C
        DO 200 N=1,NUMEL
        AREA=(AJ(N)*BK(N)-AK(N)*BJ(N))*.5
        COMM=.25*ET(N)/((1.-XU(N)**2)*AREA)
        A(1,1)=BJ(N)-BK(N)
        A(1,2)=0.0
        A(1,3)=BK(N)
        A(1,4)=0.0
        A(1,5)=-BJ(N)
        A(1,6)=0.0
        A(2,1)=0.0
        A(2,2)=AK(N)-AJ(N)
        A(2,3)=0.0
        A(2,4)=-AK(N)
        A(2,5)=0.0
        A(2,6)=AJ(N)
        A(3,1)=AK(N)-AJ(N)
        A(3,2)=BJ(N)-BK(N)
        A(3,3)=-AK(N)
        A(3,4)=BK(N)
        A(3,5)=AJ(N)
        A(3,6)=-BJ(N)
        B(1,1)=COMM
        B(1,2)=COMM*XU(N)
        B(1,3)=0.0
        B(2,1)=COMM*XU(N)
        B(2,2)=COMM
        B(2,3)=0.0
        B(3,1)=0.0
        B(3,2)=0.0
        B(3,3)=COMM*(1.-XU(N))*.5
C
        DO 182 J=1,6
        DO 182 I=1,3
        S(I,J)=0.0
```

```
      DO 182 K=1,3
  182 S(I,J)=S(I,J)+B(I,K)*A(K,J)
      DO 183 J=1,6
      DO 183 I=1,3
  183 B(J,I)=S(I,J)
      DO 184 J=1,6
      DO 184 I=1,6
      S(I,J)=0.0
      DO 184 K=1,3
  184 S(I,J)=S(I,J)+B(I,K)*A(K,J)
C
      LM(1)=NPI(N)
      LM(2)=NPJ(N)
      LM(3)=NPK(N)
      DO 200 L=1,3
      DO 200 M=1,3
      LX=LM(L)
      MX=0
  185 MX=MX+1
      IF(NP(LX,MX)-LM(M)) 190,195,190
  190 IF(NP(LX,MX)) 185,195,185
  195 NP(LX,MX)=LM(M)
      IF (MX-10) 196,702,702
  196 SXX(LX,MX)=SXX(LX,MX)+S(2*L-1,2*M-1)
      SXY(LX,MX)=SXY(LX,MX)+S(2*L-1,2*M)
      SYX(LX,MX)=SYX(LX,MX)+S(2*L,2*M-1)
  200 SYY(LX,MX)=SYY(LX,MX)+S(2*L,2*M)
C
C     COUNT OF ADJACENT NODAL POINTS
C
      DO 206 M=1,NUMNP
      MX =1
  205 MX=MX+1
      IF (NP(M,MX)) 206,206,205
  206 NAP(M)=MX-1
C
C     INVERSION OF NODAL POINT STIFFNESS
C
      DO 210 M=1,NUMNP
      COMM=SXX(M,1)*SYY(M,1)-SXY(M,1)*SYX(M,1)
      TEMP=SYY(M,1)/COMM
      SYY(M,1)=SXX(M,1)/COMM
      SXX(M,1)=TEMP
      SXY(M,1)=-SXY(M,1)/COMM
  210 SYX(M,1)=-SYX(M,1)/COMM
C
C     MODIFICATION OF BOUNDARY FLEXIBILITIES
C
      PRINT 112
      READ  4, (NPB(L),NFIX(L),SLOPE(L),L=1,NUMBC)
      PRINT 4, (NPB(L),NFIX(L),SLOPE(L),L=1,NUMBC)
      DO 240 L=1,NUMBC
      M=NPB(L)
      NP(M,1)=0
      IF(NFIX(L)-1) 225,220,215
  215 C=(SXX(M,1)*SLOPE(L)-SXY(M,1))/(SYX(M,1)*SLOPE(L)-SYY(M,1))
      R=1.-C*SLOPE(L)
      SXX(M,1)=(SXX(M,1)-C*SYX(M,1))/R
      SXY(M,1)=(SXY(M,1)-C*SYY(M,1))/R
```

```
      SYX(M,1)=SXX(M,1)*SLOPE(L)
       SYY(M,1)=SXY(M,1)*SLOPE(L)
      GO TO 240
  220 SYY(M,1)=SYY(M,1)-SYX(M,1)*SXY(M,1)/SXX(M,1)
      GO TO 230
  225 SYY(M,1)=0.0
  230 SXX(M,1)=0.0
  235 SXY(M,1)=0.0
      SYX(M,1)=0.0
  240 CONTINUE
C
C       ITERATION ON NODAL POINT DISPLACEMENTS
C
  243 PRINT 119
  244 SUM=0.0
      DO 290 M=1,NUMNP
      NUM=NAP(M)
      IF (SXX(M,1)+SYY(M,1)) 275,290,275
  275 FRX=XLOAD(M)
      FRY=YLOAD(M)
      DO 280 L=2,NUM
      N=NP(M,L)
      FRX=FRX-SXX(M,L)*DSX(N)-SXY(M,L)*DSY(N)
  280 FRY=FRY-SYX(M,L)*DSX(N)-SYY(M,L)*DSY(N)
      DX=SXX(M,1)*FRX+SXY(M,1)*FRY-DSX(M)
      DY=SYX(M,1)*FRX+SYY(M,1)*FRY-DSY(M)
      DSX(M)=DSX(M)+XFAC*DX
      DSY(M)=DSY(M)+XFAC*DY
      IF (NP(M,1)) 285,290,285
  285 SUM=SUM+ABSF(DX/SXX(M,1))+ABSF(DY/SYY(M,1))
  290 CONTINUE
C
C       CYCLE COUNT AND PRINT CHECK
C
      NCYCLE=NCYCLE +1
      IF (NCYCLE-NUMPT) 305,300,300
  300 NUMPT=NUMPT+NCPIN
      PRINT 120,NCYCLE,SUM
  305 IF (SUM-TOLER) 400,400,310
  310 IF(NCYCM-NCYCLE) 400,400,315
  315 IF (NCYCLE-NUMOPT) 244,320,320
  320 NUMOPT=NUMOPT+NOPIN
C
C       PRINT OF DISPLACEMENTS AND STRESSES
C
  400 PRINT 99
      PRINT 100
      PRINT 121
      PRINT 122,(NPNUM(M),DSX(M),DSY(M),M=1,NUMNP)
      PRINT 123
      DO 420 N=1,NUMEL
      I=NPI(N)
      J=NPJ(N)
      K=NPK(N)
      EPX=(BJ(N)-BK(N))*DSX(I)+BK(N)*DSX(J)-BJ(N)*DSX(K)
      EPY=(AK(N)-AJ(N))*DSY(I)-AK(N)*DSY(J)+AJ(N)*DSY(K)
      GAM= (AK(N)-AJ(N))*DSX(I)-AK(N)*DSX(J)+AJ(N)*DSX(K)
     1   +(BJ(N)-BK(N))*DSY(I)+BK(N)*DSY(J)-BJ(N)*DSY(K)
      COMM=ET(N)/((1.-XU(N)**2)*(AJ(N)*BK(N)-AK(N)*BJ(N)))
```

```
      X=COMM*(EPX+XU(N)*EPY)+THERM(N)
      Y=COMM*(EPY+XU(N)*EPX)+THERM(N)
     XY=COMM*GAM*(1.-XU(N))*.5
     SIGXX(N)=X
     SIGYY(N)=Y
     SIGXY(N)=XY
     C=(X+Y)/2.0
     R=SQRTF(((Y-X)/2.0)**2+XY**2)
     XMAX=C+R
     XMIN=C-R
     PA=0.5*57.29578*ATANF ( 2.* XY/(Y-X))
     IF (2.*X-XMAX-XMIN) 405,420,420
 405 IF (PA) 410,420,415
 410 PA=PA+90.0
     GO TO 420
 415 PA=PA-90.0
 420 PRINT 124, (NUME(N),X,Y,XY,XMAX,XMIN,PA)
C
     PRINT 823
     DO 900  M=1,NUMNP
      X=0.0
      Y=0.0
     XY=0.0
     SRX=0.0
     SRY=0.0
     R=0.0
     DO 860 N=1,NUMEL
     I=NPI(N)
     J=NPJ(N)
     K=NPK(N)
     IF (M-I) 830,850,830
 830 IF (M-J) 835,845,835
 835 IF (M-K) 860,840,860
 840 I=NPK(N)
     K=NPI(N)
     GO TO 850
 845 I=NPJ(N)
     J=NPI(N)
 850 A=ABSF(XORD(J)+XORD(K)-2.*XORD(I))
     B=ABSF(YORD(J)+YORD(K)-2.*YORD(I))
     RY=B/(A+B)
     SRY=SRY+RY
     Y=Y+SIGYY(N)*RY
     RX=A/(A+B)
     SRX=SRX+RX
     X=X+SIGXX(N)*RX
     R=R+1.0
     XY=XY+SIGXY(N)
 860 CONTINUE
     X=X/SRX
     Y=Y/SRY
     XY=XY/R
     C=(X+Y)/2.0
     R=SQRTF(((Y-X)/2.0)**2+XY**2)
     XMAX=C+R
     XMIN=C-R
     PA=0.5*57.29578*ATANF ( 2.* XY/(Y-X))
     IF (2.*X-XMAX-XMIN) 805,820,820
 805 IF (PA) 810,820,815
```

```
  810 PA=PA+90.0
      GO TO 820
  815 PA=PA-90.0
  820 PRINT 124,(M,X,Y,XY,XMAX,XMIN,PA)
  900 CONTINUE
C
      IF (SUM-TOLER) 440,440,430
  430 IF (NCYCM-NCYCLE) 440,440,243
C
  440 GO TO 150
C
C     PRINT OF ERRORS IN INPUT DATA
C
  701 PRINT 711,(N)
      GO TO 440
  702 PRINT 712,(LX)
      GO TO 440
C
C       FORMAT STATEMENTS
C
    1 FORMAT (6I4,2E12.5,4I1)
    2 FORMAT (4I4,4E12.4,F8.4)
    3 FORMAT (1I4,4F8.1,2F12.8)
    4 FORMAT (2I4,1F8.3)
    5 FORMAT (3E15.8)
   99 FORMAT (1H1)
  100 FORMAT (72H  BCD INFORMATION
     1                    )
  101 FORMAT(29HONUMBER OF ELEMENTS          =1I4/)
  102 FORMAT(29H NUMBER OF NODAL POINTS      =1I4/)
  103 FORMAT(29H NUMBER OF BOUNDARY POINTS   =1I4/)
  104 FORMAT(29H CYCLE PRINT INTERVAL        =1I4/)
  105 FORMAT(29H OUTPUT INTERVAL OF RESULTS  =1I4/)
  106 FORMAT(29H CYCLE LIMIT                 =1I4/)
  107 FORMAT(29H TOLERANCE LIMIT             =1E12.4/)
  108 FORMAT(29H OVER RELAXATION FACTOR      =1F6.3)
  109 FORMAT (1I8,4F12.1,2F12.8)
  110 FORMAT (74H1EL.    I   J   K        E         DENSITY      POISSON
     1  ALPHA      DELTA T)
  111 FORMAT (80H1      NP        X-ORD        Y-ORD       X-LOAD       Y-LOA
     1D       X-DISP       Y-DISP)
  112 FORMAT (20H BOUNDARY CONDITIONS)
  119 FORMAT(34H0         CYCLE     FORCE UNBALANCE)
  120 FORMAT (1I12,1E20.6)
  121 FORMAT (42HONODAL POINT X-DISPLACEMENT Y-DISPLACEMENT)
  122 FORMAT (1I12,2E15.6)
  123 FORMAT(120H1  ELEMENT              X-STRESS              Y-STRESS
     1       XY-STRESS           MAX-STRESS     MIN-STRESS        DIRECTION)
  124 FORMAT (1I10,3F20.4,5X,3F15.2)
  711 FORMAT (32HOZERO OR NEGATIVE AREA, EL. NO.=1I4)
  712 FORMAT (33HOOVER 8 N.P. ADJACENT TO N.P. NO.1I4)
  823 FORMAT(120H1  N-POINT              X-STRESS              Y-STRESS
     1       XY-STRESS           MAX-STRESS     MIN-STRESS        DIRECTION)
C
      END
```

At the present time (Dec. 2013), this FORTRAN program should be less than 3 pages – Ed Wilson